Preparation of the Temperature-Responsive Superhydrophobic Paper with High Stability

Shangjie Jiang,* Shisheng Zhou, Bin Du, and Rubai Luo

Read Online

ACCESS | Metrics & More | Article Recommendations | Supporting Information

ABSTRACT: In this paper, a method for preparing a high-stability superhydrophobic paper with temperature-induced wettability transition is proposed. First, a temperature-responsive superhydrophobic triblock polymer PHFMA−PTSPM−PNIPAAm was prepared by one-step polymerization of TSPM, HFMA, and NIPAAm in a mass ratio of 0.3:0.3:0.3, then a superhydrophobic paper with a good temperature response was successfully prepared by grafting amino-modified SiO_2 with the polymer to modify the surface of the paper. A further study found that when the mass ratio of amino-modified SiO_2 to polymer is 0.2, the coating has good superhydrophobicity and transparency. What is more, the prepared modified paper is in a superhydrophobic state when the temperature is higher than 32 °C, and is in a superhydrophilic state when it is lower than 32 °C, which can realize free conversion between superhydrophobic and superhydrophilic states. In addition, the superhydrophobic paper prepared by this method not only has high oil−water separation efficiency, and the superhydrophobic coating shows good stability and transparency, but also has low requirements of environmental conditions for preparation, relatively simple preparation process, and strong repeatability, and it has a very broad application prospect.
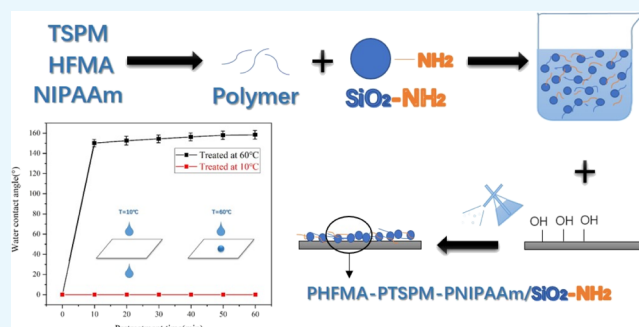
1. INTRODUCTION

Superhydrophobic materials with an intelligent response are materials that control the wettability transformation of a material surface through physical change or chemical reaction under external stimulation,[1−4] and environmental stimulus-sensitive superhydrophobic surfaces have become a hot area of academic research.[5] Studies have found some common environmentally responsive superhydrophobic surfaces, such as light response, temperature response, pH response, electric field response, ionic liquid response, and magnetic response.[6−14] Nowadays, a lot of waste oil and water mixtures are produced in the industrial production process, and superhydrophobic materials can not only separate these mixtures through filtration or single-phase selective absorption, but also realize the free switching of oil−water separation according to production needs in different external environments, which shows their strong industrial application value. Therefore, the preparation of intelligent responsive materials has become an important issue of industrial production.[15−18] However, due to the high cost and complex preparation process, their application value in industrial production is limited to a certain extent.[19,20] After experimental research and practical verification, it is gradually found that temperature-responsive superhydrophobic surfaces have the advantages of a fast response, low requirement of preparation equipment, and simple preparation process, which make them show a greater production and application value and also set off an upsurge of

academic research on temperature-responsive superhydrophobic surfaces.[21,22]

From the existing research, many temperature-responsive superhydrophobic surface preparation methods have been proposed, but these methods still have certain limitations. First, by drip-coating PCL solution (poly-ε-caprolactone) on a substrate with a certain array structure to form a film on the surface, a reversible temperature conversion superhydrophobic surface with a critical temperature of 60 °C is obtained. Or free radical polymerization was used to react capric acid with butyl phthalate, immersing the fiber in the reactant to obtain a low surface energy, and then silica was used for roughness modification to obtain an intelligent superhydrophobic surface with pH control. However, due to the lack of adhesion between the polymer prepared by this method and the rough surface, the stability of the superhydrophobic surface is not high.[23,24] Second, by grafting temperature-sensitive organics onto a silica gel substrate with an array of nanopillars, the distance and width of the protrusions are controlled to affect

the temperature change, thereby realizing the reversible conversion of superhydrophobicity and superhydrophilicity. However, in this method, due to the poor flexibility of the substrate, the difficulty of processing, the lack of recyclability and degradability, etc., to a certain extent, its application value in production is limited.[25] Third, the rough surface was constructed by layer by layer self-assembly of nano-SiO_2 and polyacrylamide salt on the substrate. Then, a single layer of fluorinated azobenzene is modified on the rough surface to obtain a surface that can realize the reversible conversion of superhydrophobicity and superhydrophilicity under ultraviolet light. However, the transparency of the coating prepared by this method is not ideal, which affects the color and light transmittance of the substrate.[26] Fourth, a strawberry-like TiO_2 film is prepared by the seed growth method, whose surface contact angle can reach 163°, which can realize the conversion of superhydrophobicity and hydrophilicity under natural light. However, from the perspective of the preparation process of this method, the reaction conditions of this method are harsh and the process is complex, and its applicability for commercial production is poor.[27]

In this study, a one-step method was used to promote the temperature-responsive monomer N-isopropylacrylamide (NIPAAm), the fluorine-containing monomer hexafluorobutyl methacrylate (HFMA), and the silicon-containing cross-linking agent 3-trimethoxysilyl propyl methacrylate (TSPM) polymerized in tetrahydrofuran solution to prepare a low surface energy triblock polymer with temperature-induced wettability transition. In order to improve the roughness of the paper and enhance the adhesion between the polymer and silica, APTES was used to aminate silica nanoparticles, and the prepared polymer and amino-modified SiO_2 were grafted in solution to obtain a temperature-responsive superhydrophobic coating, which was sprayed on the surface of the substrate to obtain a superhydrophobic paper. NIPAAm in the polymer can make the paper surface have temperature-responsive properties, and HFMA provides the low surface energy required for superhydrophobic surfaces. In the experiment, we used the silicon-containing cross-linking agent TSPM to cross-link the fluorine-containing monomer HFMA and the temperature-responsive monomer PNIPAAm to prepare high molecular polymers, and then used TSPM to graft amino-modified silica onto the polymer to improve the surface roughness of the substrate to enhance the stability of superhydrophobic properties.[28,29] This method has the advantages of simple preparation process, high efficiency, and a wide range of applications (suitable for various types of papers). The prepared temperature-responsive superhydrophobic paper not only has the advantages of light weight, easy to carry and transport, good printability, low cost, strong recyclability, and good biodegradability, but can also achieve the reversible conversion between superhydrophobic and superhydrophilic properties by changing the temperature, and the effective separation of oil−water mixtures can be achieved in the superhydrophobic state. This kind of coating surface with high transparency and high stability shows great potential for industrial applications.[30]

2. RESULTS AND DISCUSSION

2.1. Effect of the Monomer Ratio on Wettability and Responsiveness.
The influence of different proportions of HFMA, TSPM, and NIPAAm on the wettability and response performance of the paper was explored. In this study, the polymer was synthesized in three proportions and then grafted

with amino-modified SiO_2, and three different superhydrophobic papers were prepared on the basis of sufficient roughness in the structure, through comparative analysis to determine the monomer ratio with the best overall performance.

The three prepared papers were pretreated at 60 °C and then the contact angle test was performed. It can be seen from Table 1 that when the ratio of HFMA, TSPM, and NIPAAm is

Table 1. Surface Contact Angle and Responsiveness of the Modified Paper Prepared with Different Monomer Ratios

	HFMA	TSPM	PIPAAm	water contact angle	responsiveness
sample 1	0.1	0.3	0.3	143 ± 2	√
sample 2	0.3	0.3	0.3	158 ± 3	√
sample 3	0.6	0.3	0.3	159 ± 1	×

0.1:0.3:0.3, the contact angle is 143 ± 2°. With the increase of the ratio of HFMA, when the ratio reaches 0.3:0.3:0.3, the contact angle is 158 ± 3°, reaching the superhydrophobic condition; and when the ratio is 0.6:0.3:0.3, the contact angle reaches 159 ± 1°.

The water contact angle of the three papers was measured under different temperature conditions to explore the effect of different monomer ratios on the response performance of the paper. When the monomer ratios of HFMA:TSPM:NIPAAm were 0.1:0.3:0.3 and 0.3:0.3:0.3, the modified paper could respond to different temperatures. When the ratio was 0.3:0.3:0.3, the paper was placed in a 60 °C environment for pretreatment, and then the contact angle test was performed at a constant temperature, the contact angle at this time is 157 ± 3°, the water droplets were spherical on the surface of the paper, the paper has superhydrophobic properties, and it remains superhydrophobic after 5 h (Figure 1a). However, after the paper was pretreated in an environment of 10 °C, the liquid droplets on the surface quickly penetrate into the paper, and the water droplets were gradually absorbed by the paper after a few seconds and spread completely on the surface within 30 s, and the paper changed from the superhydrophobic state to superhydrophilic state (the process is shown in Figure 1b). It can be seen from Figure 1a,b that the superhydrophobic paper already shows good temperature-response performance. Further research found that this transition between superhydrophilic and superhydrophobic states was completely reversible within 10 cycles (Figure 1c). When the monomer ratio HFMA:TSPM:NIPAAm was 0.6:0.3:0.3, because the fluorine atoms with low surface energy play a superhydrophobic role in the polymer, with the increase of the HFMA content, the proportion of hydrophobic blocks also increased, which makes the paper lose its responsiveness and maintain the superhydrophobic state at different temperatures.

Based on the above research results, it can be found that the proportion of fluorine-containing monomer is the main factor affecting the hydrophobicity of the coating. However, when the block ratio is too high, the responsiveness of the coating surface will decrease or even lose responsiveness. Considering hydrophobic performance and response performance comprehensively, the best ratio of HFMA:TSPM:NIPAAm was found to be 0.3:0.3:0.3 in this experiment.

2.2. Accurate Control of Roughness.
In general, the superhydrophobic modification of the paper will not only change the wettability of the paper, but also change the color,
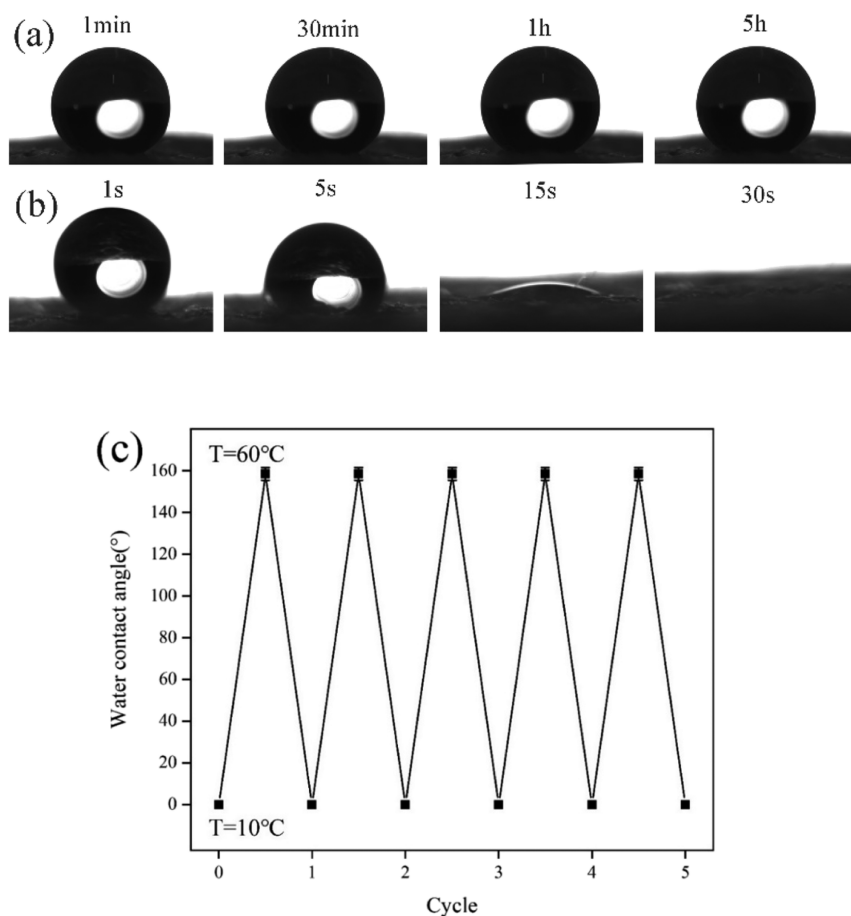
Figure 1. When the monomer ratio of HFMA:TSPM:NIPAAm is 0.3:0.3:0.3, the contact angle change of the paper at different temperatures was measured: (a) $T = 60\ °C$, (b) $T = 10\ °C$, and (c) reversible conversion of superhydrophilic and superhydrophobic properties of the paper surface at 10 °C and 60 °C.

and the relevant studies have also found that the content of SiO$_2$ will directly affect the transparency and superhydrophobicity of the coating.[31] Figure 2a shows the direct relationship between the superhydrophobicity (test the water contact angle under superhydrophobic conditions, i.e., $T = 60\ °C$) and color difference (color difference from the original paper) of several modified papers prepared under different mass ratios of amino-modified SiO$_2$ and temperature-responsive polymers. Figure 2b shows the reflectance spectra of three papers prepared with amino-modified SiO$_2$ and polymer under different mass ratios. While testing the reflectance spectra of the three papers, the L, a, and b values of the three are also tested (L, a, and b represent the chromaticity value of the object color, L represents brightness, a represents red-green, and b represents yellow-blue), the L^*, a^*, and b^* values, quantitatively characterizing the color of the samples, are reported in Table S1. Figure 2c shows the scanning electron microscopy (SEM) image of the fiber on the surface of the paper. It can be seen from the figure that the surface roughness of the paper increases with the increase of the content of amino-modified silica. Specifically, in Figure 2a, curve A1 shows the effect of the SiO$_2$ content on the contact angle, and curve A2 shows the color difference ΔE caused by the SiO$_2$ content on paper surface. It can be seen from Figure 2a that as the content of SiO$_2$ increases within a certain range, the surface of the paper will become rougher. While the superhydrophobic properties of the paper are significantly improved, it also affects the light

transmittance of the coating and the color of the paper surface, so that the chromatic aberration ΔE of the paper also increases. When SiO$_2$ is not added, the contact angle of the paper surface is about 90°, and the fiber surface is smooth and flat (Figure 2c(I)). When the ratio of the SiO$_2$ to polymer content is 0.1, the paper has poor hydrophobicity due to the insufficient surface roughness, and the contact angle is lower than 150° (the surface of the paper fiber is shown in Figure 2c(II)). When the ratio of the SiO$_2$ to polymer content is 0.2, the paper surface obtains sufficient roughness (the surface of the paper fiber is shown in Figure 2c(III)), the contact angle at this time is greater than 150°, and the paper obtains superhydrophobic properties. The reflectance spectrum is shown as curve B2 in Figure 2b, compared with the reflectance spectrum curve B1 of the original paper, the treated paper has a similar spectral reflectance in the range of 400−600 nm, a slight deviation in the red spectral region of 600−700 nm, and the measured color difference is $\Delta E = 0.91$. When the ratio of the SiO$_2$ to polymer content reaches 0.3, the SEM image of the paper fiber is shown in Figure 2c(IV). Compared with a silica content ratio of 0.2, although the change in the contact angle of the paper surface is very small at this time, the color difference is $\Delta E = 1.58$, which has exceeded the acceptable color difference range of the human eye ($\Delta E < 1$).[32] At this time, the reflective recording curve is shown as B3 in Figure 2b, and its deviation from the reflectance spectrum curve B1 of the original paper in the 400−600 nm red spectral region is
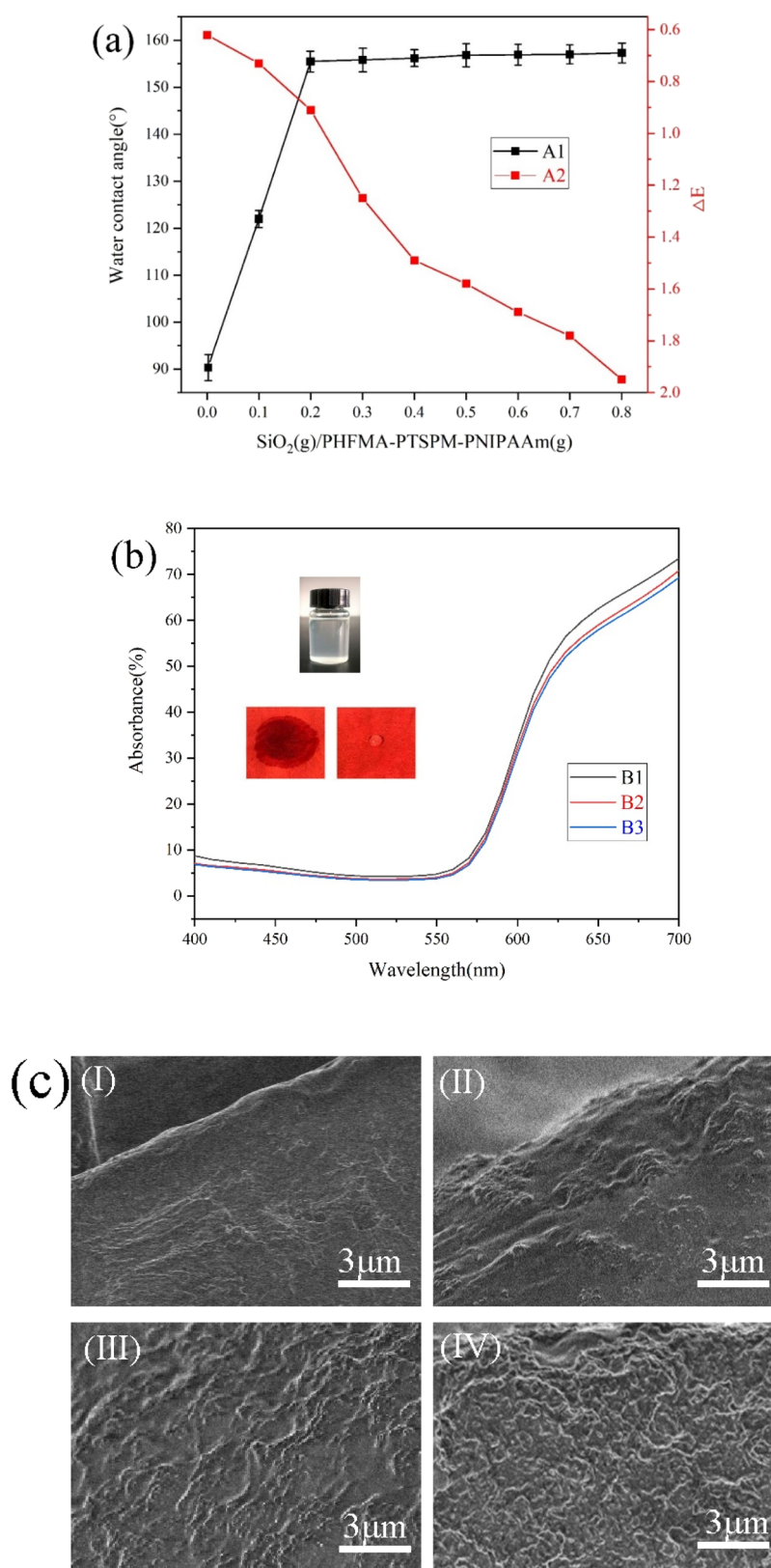
Figure 2. Characterization of the superhydrophobic paper prepared with amino-modified SiO₂ and polymer under different mass ratios: (a) contact angle and chromatic aberration, (b) reflectance spectrum, (c) SEM images under different mass ratios: (I) 0, (II) 0.1, (III) 0.2, and (IV) 0.3.

greater. Therefore, according to Figure 2a,b, the best mass ratio of amino-modified SiO₂ to polymer was found to be 0.2.

2.3. Structure Characterization. Figure 3 shows the infrared spectra of TSPM, temperature-responsive polymer PHFMA−TSPM−NIPAAm, amino-modified SiO₂, temperature-responsive superhydrophobic PHFMA−TSPM−NIPAAm/SiO₂−NH₂ coating. Curve a is the infrared spectrum of TSPM. As can be seen from the figure, 2945 cm⁻¹ is the
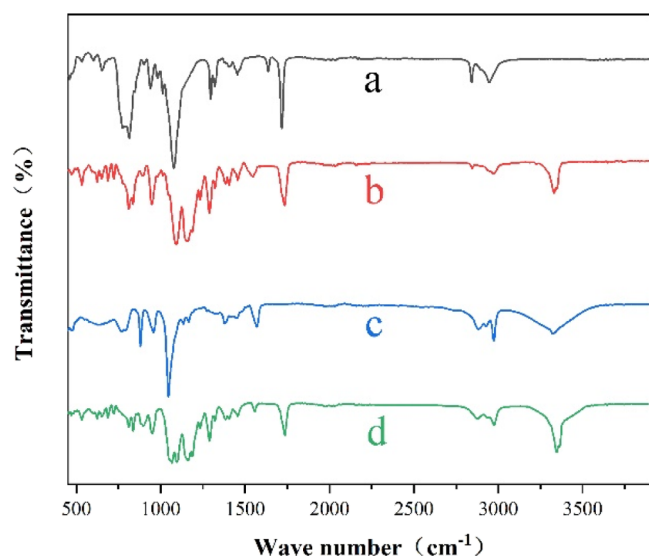
Figure 3. Fourier infrared spectrum analysis chart: (a) TSPM, (b) temperature-responsive polymer PHFMA−PTSPM−PNIPAAm, (c) amino-modified SiO_2, and (d) temperature-responsive superhydrophobic coating PHFMA−PTSPM−PNIPAAm/SiO_2−NH_2.

stretching vibration absorption peak of the methyl group, 2841 cm^{-1} is the characteristic stretching vibration absorption peak of the methylene group, 1720 cm^{-1} is the stretching vibration absorption peak of C=O, and 1638 cm^{-1} is the stretching vibration peak of C=C, the symmetrical stretching vibration peak of Si−C appears at 813 cm^{-1}, and the stretching vibration peak of Si-OC appears at 1078 cm^{-1}. Curve b is the infrared spectrum of the polymer PHFMA−PTSPM−NIPAAm. In addition to the characteristic peaks of the curve a, the stretching vibration absorption peak of CF appears at 1160 cm^{-1}, the peaks appearing at 3298 and 1546 cm^{-1} are caused by the stretching and bending vibrations of the N−H peak in the amide of NIPAAm, and the characteristic peak of C=C disappears at 1638 cm^{-1}, the changes in the infrared spectrum confirm the synthesis of the polymer PHFMA−PTSPM−PNIPAAm. Curve c is the infrared spectrum of amino-modified silica. As can be seen from the figure, 1051 cm^{-1} is the antisymmetric stretching vibration peak of Si−O−Si, the characteristic absorption peaks of methyl and methylene stretching vibration appear at 2973 and 2880 cm^{-1}, respectively, at 1549 cm^{-1} is the flexural vibration peak of NH, and the broad peak near 3300 cm^{-1} is caused by the stretching vibration of N−H, the appearance of the above peaks proves the modification of silica. Curve d is the infrared
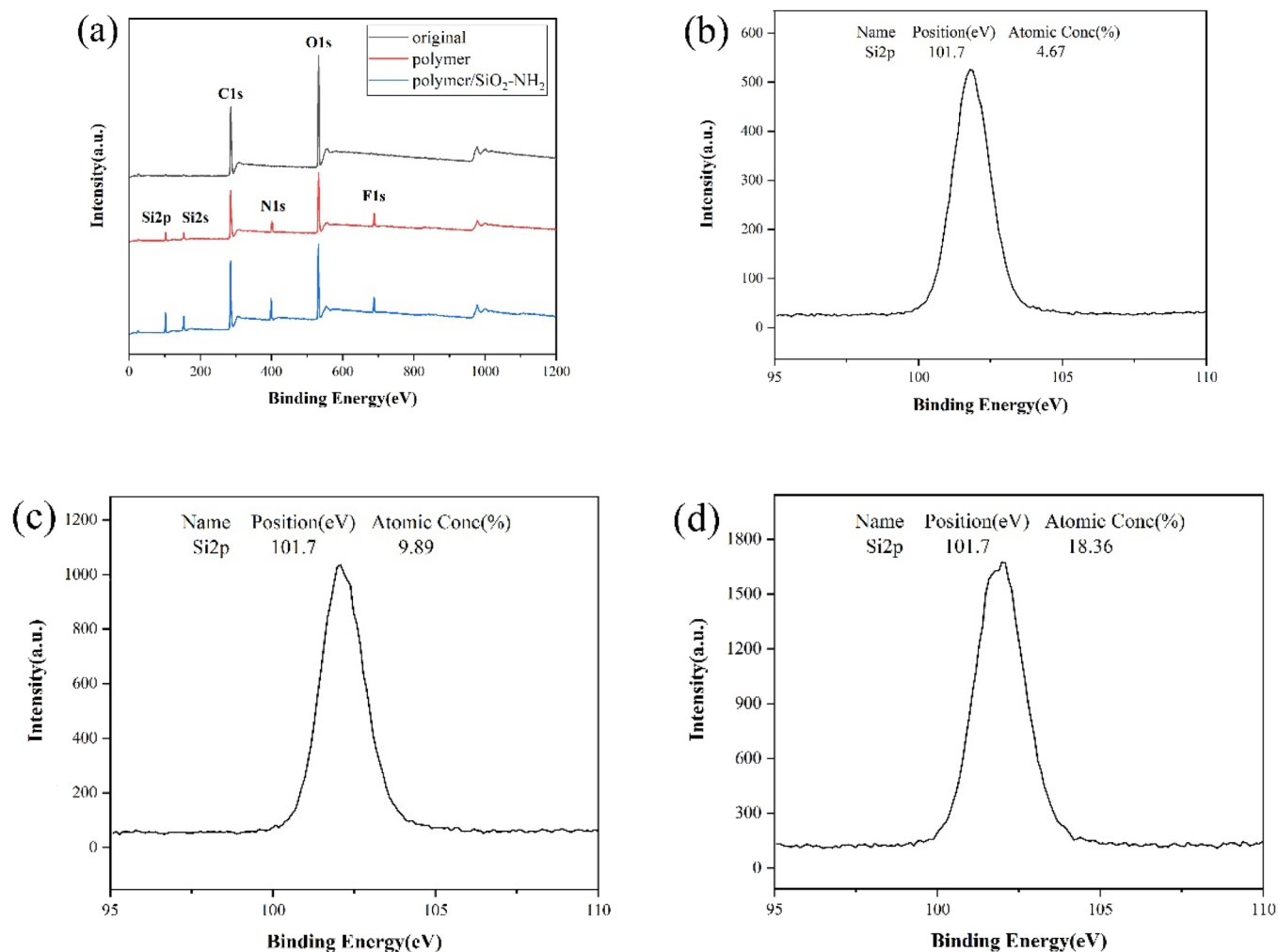

Figure 4. (a) XPS analysis chart; XPS Si 2p core level spectra of (b) original paper, (c) PHFMA−PTSPM−PNIPAAm-coated paper, and (d) PHFMA−TSPM−NIPAAm/SiO_2−NH_2-coated paper.

spectrum of the PHFMA−PTSPM−PNIPAAm/SiO_2−NH_2 coating. The stretching vibration peak of Si−O−C can be observed at 1078 cm^{-1}, the stretching vibration peak of C−F can be observed at 1160 cm^{-1}, the antisymmetric stretching vibration peak of Si−O−Si in amino-modified SiO_2 can be observed at 1051 cm^{-1}, and the bending vibration peak and stretching vibration peak of N−H can be observed at 1550 and 3290 cm^{-1}, respectively. The characteristic peaks of curves b and c seen in the figure can basically be observed in the Fourier transform infrared (FTIR) spectrum of the response polymer of the composite PHFMA−PTSPM−PNIPAAm/SiO_2−NH_2, and the results of FTIR also indicate the successful synthesis and the successful introduction of amino-modified SiO_2 into polymers.[33]

The surface elements of the original paper, the modified paper coated with the polymer (PHFMA−PTSPM−PNI-PAAm), and the modified paper coated with the composite coating (PHFMA−TSPM−NIPAAm/SiO_2−NH_2) were analyzed by X-ray photoelectron spectroscopy (XPS), although XPS cannot fully describe the chemical composition of paper samples due to their rough surface, it does provide qualitative information about the chemical changes before and after modification. Figure 4a shows the XPS spectrum of the unmodified original paper. It can be seen from the figure that the surface of the original paper is mainly composed of C and O elements, corresponding to the positions near 283 and 532 eV, respectively. Four more peaks appeared at 101, 151, 396, and 689 eV on the surface of the paper coated with the copolymer, corresponding to the appearance of the Si 2p, Si 2s, N 1s, and F 1s signals, indicating that the polymer was successfully modified to the paper surface. It can be seen from Figure 4c of the coated copolymer (PHFMA−PTSPM−PNIPAAm) paper that the strength of the Si 2p peak centered at 101 eV on the paper surface is significantly stronger than that of the original paper (Figure 4b), which is mainly due to the influence of the Si element on PTSPM, thus proving the successful introduction of PTSPM. It can be seen from Figure 4d that the Si peak signal on the surface of the composite PHFMA−TSPM−NIPAAm/SiO_2−NH_2 modified paper is stronger than that of the first two papers, which is caused by the addition of SiO_2, also indicating the successful combination of PHFMA−TSPM−NIPAAm/SiO_2−NH_2 and the paper.[34]

Figure 5 shows the thermogravimetric analysis (TGA) curves of paper samples a, b, c, and d. After heating all paper samples to 700 °C, the remaining weight percentage of the unmodified original paper sample a is 0%; the remaining weight percentage of the paper sample b after spraying ordinary silica dispersion is 4.28%, this is mainly due to the residual SiO_2 in the sample; the remaining weight percentage of paper sample c sprayed with amino-modified SiO_2 increased to 7.9%, compared with the pure SiO_2 curve b, this substantial change in the weight loss rate means that APTES reacts with the hydroxyl groups on SiO_2 to form amino-modified silica. The remaining weight percentage of the paper sample d coated with the superhydrophobic coating PHFMA−R-PTSPM−PIPAAm/SiO_2−NH_2 was 6.97%, and the weight loss rate reached 93.03%. These phenomena indicate that the successful modification of modified SiO_2 and the composite of PHFMA−PTSPM−PIPAAm on the surface of amino-modified SiO_2 effectively affect the thermal stability of the material.[35]

2.4. Microscopic Morphology of Superhydrophobic Paper.
In order to more intuitively reveal the changes of the superhydrophobic paper before and after modification, the
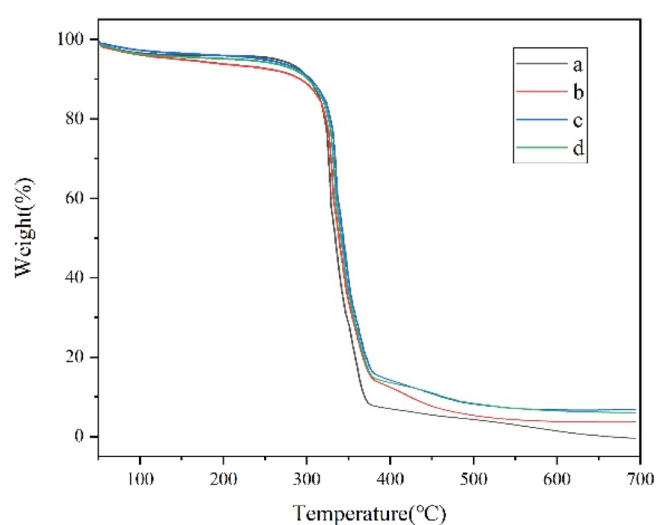

Figure 5. TGA cures of samples a, b, c, and d, (a) original paper, (b) paper coated with SiO_2, (c) paper coated with amino modified SiO_2, and (d) temperature-responsive superhydrophobic paper. Samples were heated to 700 °C in an air atmosphere at a ramp rate of 10 °C min^{-1}.

micromorphology of the paper before and after modification was compared through SEM images. In Figure 6a,c, the surface of the unmodified paper is flat and smooth, and there is no rough structure similar to protrusions. The fibers of the paper are tightly interwoven, and the gaps between the fibers are clearly visible, this reflects many excellent properties of the paper, such as good air permeability. Figure 6b,d is the modified paper fiber diagram. It can be observed from Figure 6b that the modified coating adheres uniformly, without a large amount of agglomeration and stacking, and the overall structure and shape of the fiber have not changed significantly. This indicates that the introduction of copolymers and nanoparticles not only did not destroy the structure of the fiber, but also did not have a significant impact on the paper's good air permeability and other properties. From the comparison of Figure 6c,d, it can be clearly observed that the fiber surface becomes rough due to the attachment of SiO_2 particles, which gives paper the basic conditions for super-hydrophobic properties.[36]

2.5. Determination of Critical Temperature.
The differential scanning calorimetry (DSC) curves of different monomers and temperature-responsive polymers in the experiment are shown in Figure 7. By comparing and analyzing different DSC curves, we can determine the phase transition low critical solution temperature (LCST) of temperature-responsive polymers, which is the peak point of the heat flow change during heating.[37] It can be seen from the figure that the DSC curve of HFMA has no inflection point between 25 and 45 °C, so there is no glass transition temperature in this temperature range. The peak point of NIPAAm and PHFMA−PTSPM−PNIPAAm appeared near 33 and 32 °C, respectively, in the DSC curve and the DSC curves of the polymer are similar to those of monomer NIPAAm. It can be seen from Figure 7 that there is little influence on the critical temperature change before and after polymerization, and the temperature response block is the PNIPAAm block in the polymer, which indicates that the phase transition temperature of the polymer is about 32 °C. Theoretically, when the temperature is above the LCST, the temperature-responsive polymer exhibits
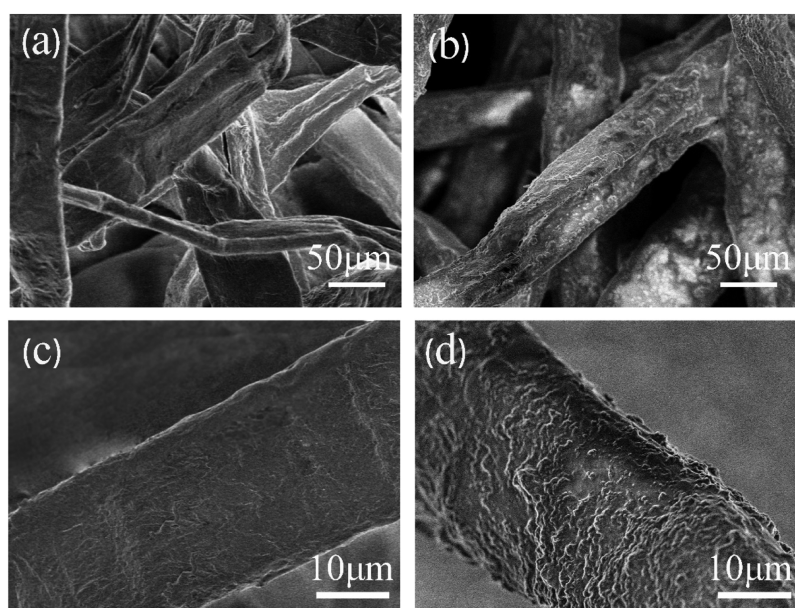
Figure 6. SEM images of the paper surface: (a) original paper and (b−d) temperature-responsive superhydrophobic paper.
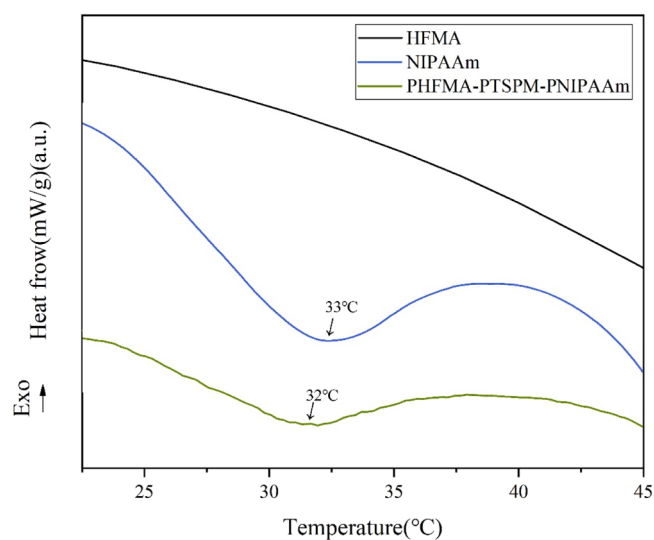

Figure 7. DSC curve of HFMA, NIPAAm, and PHFMA−PTSPM−PNIPAAm.

superhydrophobicity, and when the temperature is below the LCST, the temperature-responsive polymer exhibits hydrophilicity.[38,39]

In the experiment, we also determined the critical response temperature of the modified paper by gradually narrowing the temperature range. In the specific operation, we have prepared several oil−water mixtures at different temperatures, and observed the separation state of these oil−water mixtures by the paper. First, six identical oil−water mixtures were prepared in the beaker (50 mL oil red-stained bromobenzene and 50 mL blue deionized water), and the temperature of the oil−water mixture was adjusted in steps of 10 °C (10, 20, 30, 40, 50, and 60 °C). It can be seen from Figure 8a that when bromobenzene comes into contact with superhydrophobic paper, it quickly penetrates the surface, while water droplets can remain spherical on the surface of the paper and cannot wet the surface, the prepared paper has superhydrophobic and superlipophilic properties in this state. The device shown in Figure 8b is used to separate and collect each oil−water mixture, the process is shown in Figure 8b−e. As shown in Figure 8b, the surface of the small beaker was covered with the
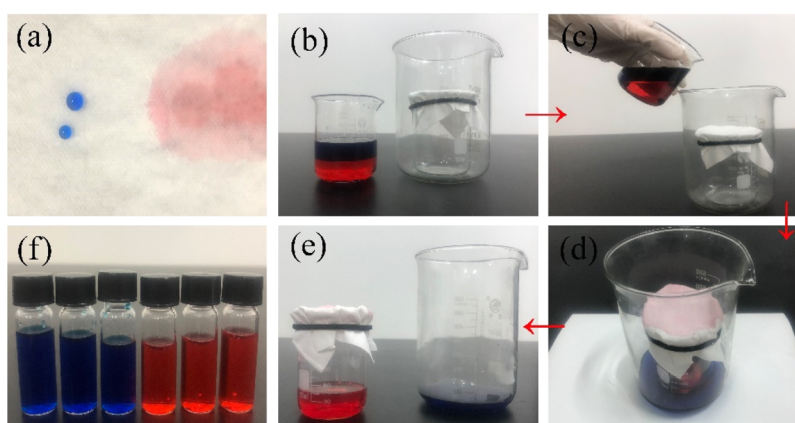

Figure 8. Oil−water separation process: (a) different wettability of modified paper to water and bromobenzene, (b−e) specific process of oil−water separation, and (f) water and bromobenzene collected after oil−water separation.
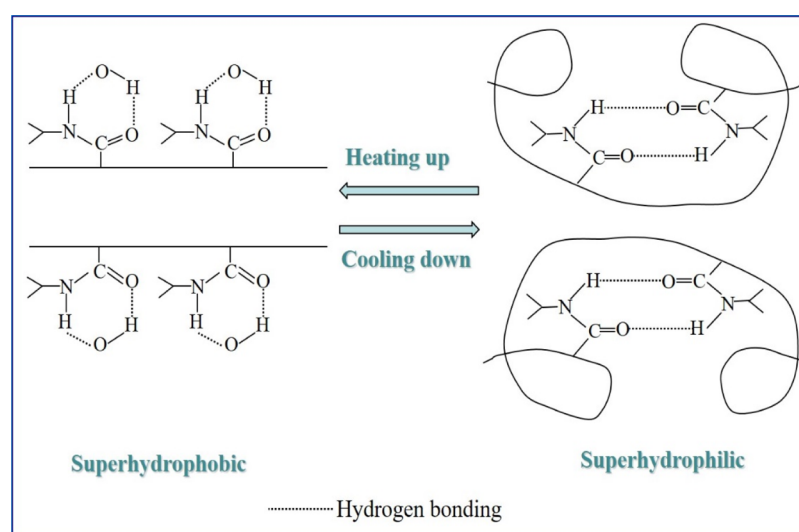
Figure 9. Mechanism of the temperature response.

modified paper and moved it to the large beaker, and slowly poured the mixture of water and bromobenzene on the surface of the paper. Due to the modified paper's superhydrophobic and lipophilic properties at a specific temperature, the organic matter in the mixture can quickly penetrate through the surface of the paper into the small beaker, while the water in the mixture stays on the surface of the paper and flows into the large beaker by gravity. When the temperature of the oil–water mixture is 10, 20, or 30 °C, the oil and water will leak into the small beaker together. At this time, the paper does not have the function of separating oil and water, which means that the paper does not have superhydrophobicity when the temperature was below 30 °C. When the temperature of the oil–water mixture is higher than 40 °C, bromobenzene dyed with oil red is collected in the small beaker, and blue deionized water is collected in the large beaker, this indicates that the paper has superhydrophobic and superlipophilic characteristics when the temperature is higher than 40 °C. Figure 8f shows bromobenzene and water collected at 40, 50, and 60 °C. Through the above experiments, it can be determined that the critical temperature range of the temperature-responsive superhydrophobic paper is 20–30 °C. In this temperature range, the temperature was adjusted with a gradient of 1 °C and repeated the above experiment to collect the oil–water separation material, and finally determined the critical temperature value. According to the test results, the critical response temperature of the prepared temperature-responsive superhydrophobic paper is 32 °C, which is consistent with the LCST value (32 °C) of the copolymer, which further shows that the modification in this study is successful.

2.6. Mechanism Analysis. As shown in Figure 9, PNIPAAm is a temperature-responsive block, the principle of temperature response is that the hydrogen bond between the amide group and the water molecule changes with different temperatures. Specifically, when the temperature is lower than the molecular LCST of PNIPAAm, the C=O and NH groups in PNIPAAm will form hydrogen bonds between molecules with external water molecules, and the molecular chain is in a stretched state. Therefore, the polymer exhibits superhydrophilic properties. In addition, the role of hydrogen bonding can cause the hydration expansion of PNIPAAm, which provides enough power for the surface segment of

PNIPAAm to cover other polymers, so that PNIPAAm dominates, which also greatly enhances its hydrophilic properties. When the temperature is higher than the LCST of PNIPAAm, the hydrogen bond between the molecules will gradually weaken as the temperature increases, making the hydrophobic interaction between isopropyl groups more obvious. Especially when the temperature increases to a certain level, the hydrogen bonds between the C=O and N–H groups and water molecules will break, forming intramolecular hydrogen bonds. Compared with the state when it is under LCST, PNIPAAm at this time will shrink and cause it to be dehydrated and collapsed, which will expose the hydrophobic groups and other hydrophobic polymers used in the polymerization reaction, such as HFMA, etc., so that the prepared polymer surface exhibits superhydrophobic characteristics.[40−42]

2.7. Stability Test. In practical applications, superhydrophobic materials will not only be corroded by various solutions, but will also suffer abrasion due to various pressures or mechanical damage. Therefore, the corrosion resistance and abrasion resistance of the superhydrophobic paper must be considered. Figure 10a,b respectively, shows the influence of acid, alkali and salt solution immersion, and friction times on the contact angle of paper at different destruction times. The three curves in Figure 10a, respectively, represent the influence of acidic solution, alkaline solution, and salt solution on the contact angle of paper at different destruction times. Specifically, as the immersion time of hydrogen chloride solution (HCL, pH = 1), sodium hydroxide solution (NaOH, pH = 14), and sodium sulfate solution (Na$_2$SO$_4$, pH = 7) increases, the contact angle of the paper has been reduced to varying degrees, but it can still maintain good hydrophobic properties. After being soaked for 150 min, the contact angles of the three soaked papers were 155 ± 1, 151 ± 1, and 156 ± 2°, respectively. After a long period of time, the alkali solution has a greater impact on the durability of the superhydrophobic properties of the paper. This is mainly because SiO$_2$ in the coating is dissolved by sodium hydroxide solution (NaOH), which leads to the degradation of superhydrophobic property. In order to test the abrasion resistance of the paper, sandpaper was pasted on the bottom of the weight, and then the friction experiment was carried out on the paper (Figure 10b). It is
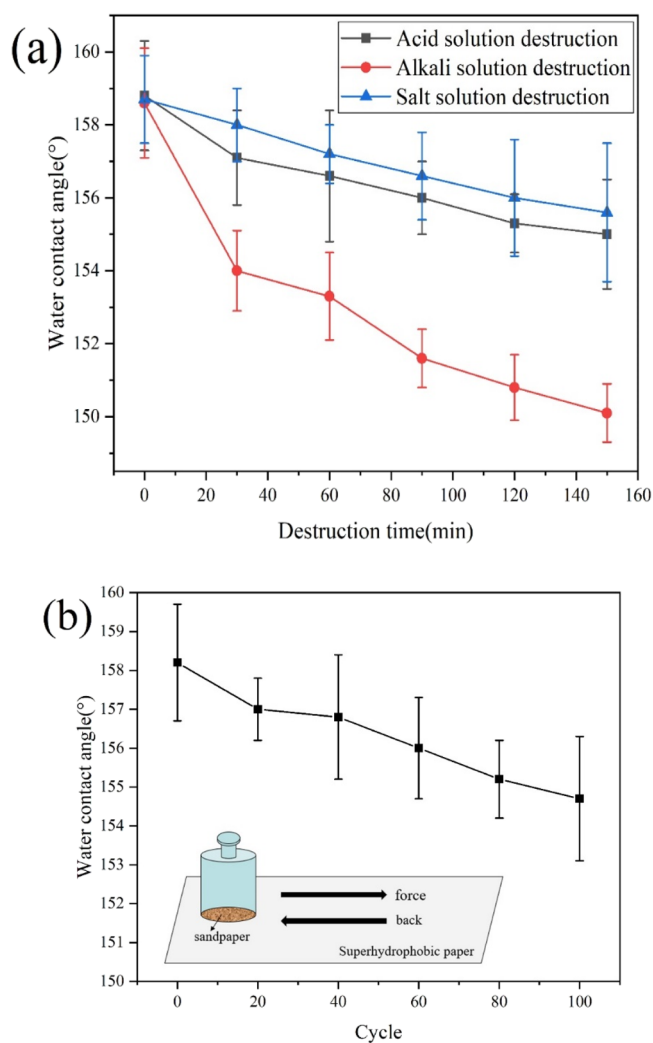
Figure 10. Effect of different destruction conditions on the contact angle of the superhydrophobic paper: (a) effect of soaking in HCL, NaOH, and Na_2SO_4 solutions on the contact angle of the paper and (b) effect of 100 friction cycles on the contact angle of the paper.

defined as a cycle that the weight is pushed to the front end of the paper and then pulled back to the original position. After the amino-modified silica is grafted with the polymer PHFMA−PTSPM−PNIPAAm and modified on the paper, a uniform and stable coating was formed on the surface of the paper covered by the polymer, so the superhydrophobic paper showed strong friction resistance in the experiment. With the increase of friction times, the paper contact angle decreases and changes little. After 100 friction cycles, the paper can still maintain a contact angle of $155 \pm 2°$. Therefore, the superhydrophobic paper has good friction resistance.

2.8. Oil−Water Separation Performance Test. The device shown in Figure 11a was used to carry out the oil−water separation experiment, the test was carried out at 60 °C, and the oil−water separation performance was analyzed. In the study, 45 mL of organic matter stained with oil red O was mixed with 45 mL of deionized water stained with methylene blue to prepare an oil−water mixture, and further analyze the separation performance of the modified superhydrophobic paper for different oil−water mixtures. The oil−water separation efficiency and recycling use are used to characterize the oil−water separation performance of the prepared

superhydrophobic paper. The separation efficiency is calculated by the following formula

$$\eta = V_1/V_0 \times 100\%$$

V_1 is the volume of oil collected after an oil−water separation experiment is completed and V_0 is the initial volume of oil before the separation experiment.

Take 1,2-dichloroethane as an example, fix the modified paper in the middle of two glassware, and pour the 60 °C mixture of 1,2-dichloroethane, bromobenzene, chloroform, and deionized water into the upper part of the container. Due to the hydrophobicity and lipophilicity of the modified paper, 1,2-dichloroethane quickly permeated the paper and flowed into the containers below, while deionized water remained on the modified paper, thus completing the separation of oil−water mixture (Figure 11a).

The oil−water separation efficiency was calculated using the above formula. It can be seen from Figure 11b that the separation efficiency of the modified paper for various oil−water mixtures such as 1,2-dichloroethane, bromobenzene, and chloroform can reach more than 98%. In addition, due to the oil−water separation process, the silica and low surface energy polymers on the paper surface will be partially dissolved in the organic solution, and some organic impurities will block the gaps between the paper fibers during the oil−water separation process, and the separation efficiency of the paper also decreases as the number of oil−water separation cycles increases. However, we are pleased that the oil−water separation efficiency of the paper prepared in this study does not decrease significantly with the increase of recycling times, and our experiments have found that the modified paper can still maintain a separation efficiency of over 96.4% after being recycled 40 times (Figure 11c).

3. CONCLUSIONS

In this study, a one-step method was used to prepare a temperature-responsive superhydrophobic triblock polymer PHFMA−PTSPM−PNIPAAm by polymerizing the monomers HFMA, TSPM, and NIPAAm in a mass ratio of 0.3:0.3:0.3, then the amino-modified SiO_2 was grafted with the polymer to modify the surface of the paper, thus a superhydrophobic paper with a good temperature response was successfully prepared. When the mass ratio of amino-modified SiO_2 to polymer is 0.2, the coating has good superhydrophobicity and transparency. The prepared modified paper is in a superhydrophobic state when the temperature is higher than 32 °C, and is in a superhydrophilic state when it is lower than 32 °C, which can realize free conversion between superhydrophobic properties and superhydrophilic properties. On the whole, the superhydrophobic paper prepared by this method not only has high oil−water separation efficiency, and that the superhydrophobic coating shows good stability and transparency, but also has low requirements of environmental conditions for preparation, a relatively simple preparation process, and strong repeatability, and it has a very broad application prospect in the fields of oil−water separation in actual industrial production.

4. EXPERIMENTAL SECTION

4.1. Materials. The main experimental materials used in this study are as follows: TSPM, HFMA (Xuejia Fluorosilicone), NIPAAm, sodium bisulfite ($NaHSO_3$), tetrahydrofuran (AIBN), aluminum oxide, potassium bromide, 1,2-dichloro-
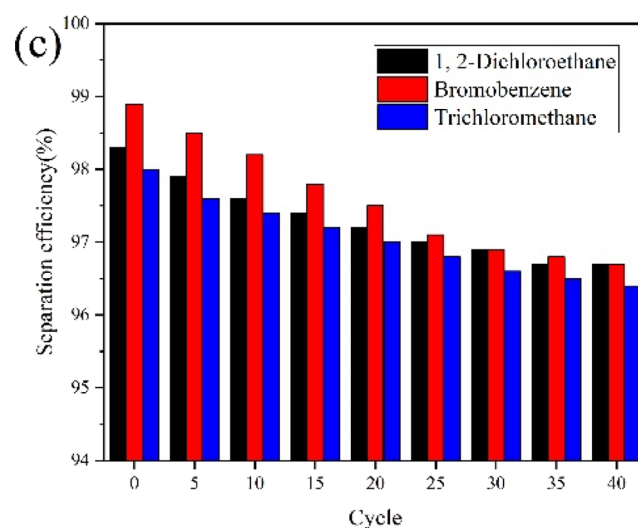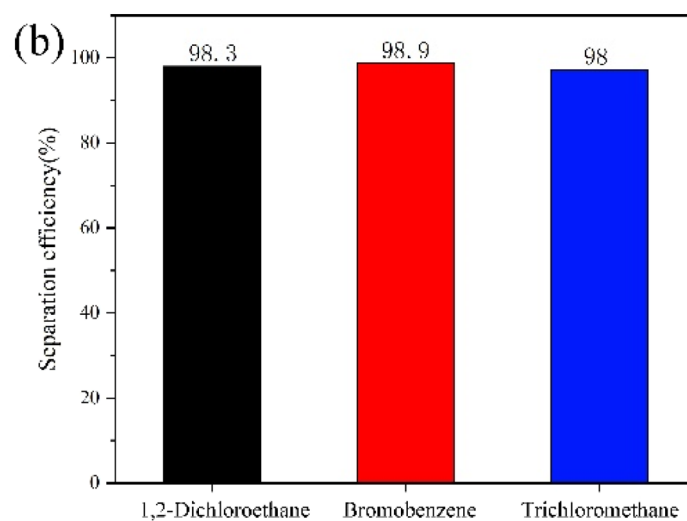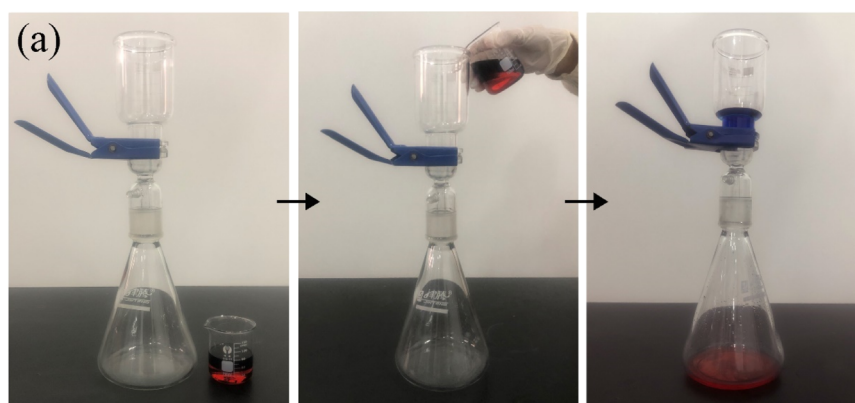
Figure 11. (a) Schematic diagram of the paper oil−water separation process, (b) separation efficiency of the paper for different oil−water mixtures, and (c) paper separation efficiency changes with the number of separations.

ethane, bromobenzene, chloroform, nano silica (Aladdin), azobisisobutyronitrile (AIBN) (Four Hevi), anhydrous ethanol (Miura), APTES (Union Silicon), and triethylamine (Tianli). All of these chemicals are not further purified before use.

4.2. Preparation of Temperature-Responsive Super-hydrophobic Copolymers. First of all, the TSPM was filtered with an alumina chromatography column to remove the polymerization inhibitor. Then, 150 g of tetrahydrofuran
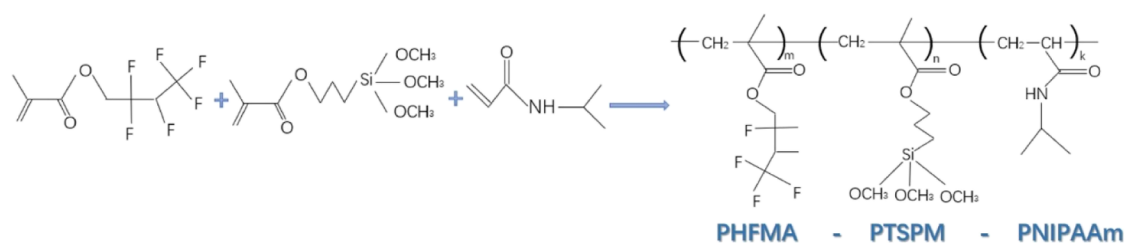
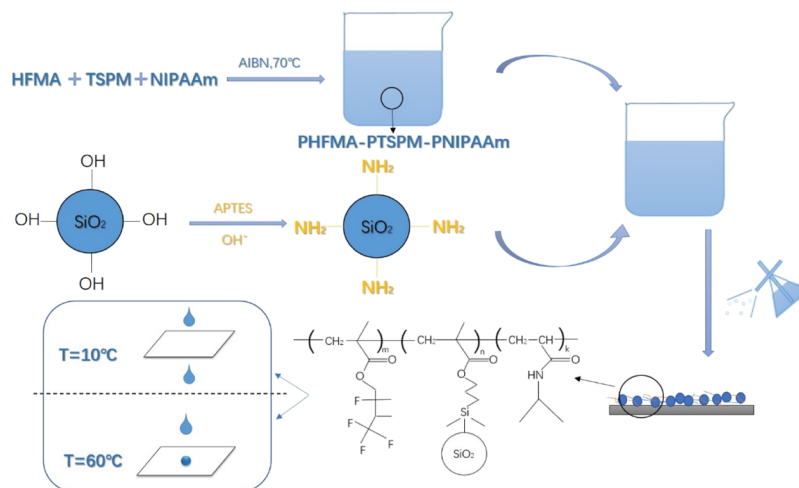**Figure 12.** Synthetic route of polymer PHFMA−PTSPM−PNIPAAm.

Figure 13. Preparation process and response performance of temperature-responsive superhydrophobic paper.

was added to the flask, and TSPM, HFMA, NIPAAm, AIBN (1.5 g), and NaHSO$_3$ (1.5 g) were added to the flask, respectively, and nitrogen was introduced into the bottle for deoxidation, which provides an oxygen free environment for the preparation of polymer. Finally, the flask was sealed and placed in a 70 °C water bath, heated, and magnetically stirred for 4 h. After the reaction, the solution was kept at room temperature, and the temperature-responsive superhydrophobic triblock polymer PHFMA−PTSPM−PNIPAAm was obtained after volatilizing the tetrahydrofuran solvent (the synthetic route of PHFMA−PTSPM−PNIPAAm is shown in Figure 12).

4.3. Preparation of Amino-Modified Nano-SiO$_2$. First of all, ethanol (200 mL) and SiO$_2$ (5 g) were added into the beaker for ultrasonic dispersion to obtain silica ethanol dispersion. Then, triethylamine was added dropwise to the beaker to reach an alkaline environment (pH = 9), and the coupling agent APTES (5 g) was added in a water bath to heat at 80 °C and magnetically stirred for 6 h to obtain an amino-modified SiO$_2$ dispersion. Finally, the obtained dispersion was centrifuged at 3000 rpm for 30 min, and the precipitate was washed with anhydrous ethanol and dried to obtain purified amino-modified SiO$_2$. Furthermore, the purified amino-modified SiO$_2$ was dried at 80 °C for 12 h and then ground to obtain powdered amino-modified nano-SiO$_2$.

4.4. Preparation of Temperature-Responsive Super-hydrophobic Paper. The prepared polymer PHFMA−PTSPM−PNIPAAm was dissolved in tetrahydrofuran, amino-modified SiO$_2$ was added, and magnetically stirred at room temperature for 1 h to form a uniform and stable temperature super-responsive hydrophobic coating (PHFMA−PTSPM−NIPAAm-SiO$_2$). Then, the coating was sprayed on a cut-out paper of 5 cm × 5 cm (the paper is German Duni brand wood

pulp paper, the size of the original paper is 40 cm × 40 cm, the weight of a single sheet is about 9.5 g, the gram weight is 60 g, the thickness is 0.48 mm, and the surface smoothness is about 87 s), and dried at 85 °C for 2 h to obtain the superhydrophobic paper. The reaction process is shown in Figure 13.

4.5. Characterization. The contact angle and rolling angle were measured with the contact angle measuring instrument DS100, and each sample was measured at 10 different points and then the average value was taken. SEM images were measured using a JSM-6701F field emission scanning electron microscope, and the sample was sprayed with gold before observing the microscopic morphology. The FT-IR test was carried out using a Bruker VECTOR-22 infrared spectrometer. An X-ray photoelectron spectrometer (Axis Ultra) was used to carry out the XPS test, using Al/Kα (1486.71 eV) as the ray, running under the conditions of 10 mA and 10 kV. The TGA of the sample was carried out with the STA449CTG thermogravimetric analyzer, which was selected to be carried out in an air atmosphere, and the heating rate was 10 °C/min. The reflectance spectrum was obtained using an integrating sphere spectrophotometer, and the test wavelength range was 400−700 nm. In the acid and alkali resistance test, the treated paper was immersed in each 0.01 g/mL HCl solution, Na$_2$CO$_3$ solution, and NaOH solution, and the soaked paper was taken out at different soaking times and then rinsed with deionized water to remove the solution. After drying the paper, five different points were randomly selected to measure the contact angle, and recorded the average value. In the abrasion resistance test, after sticking sandpaper on the bottom of a 500 g weight, rubbing back and forth in the horizontal direction at a speed of 2 cm/s with 20 cm as a friction length, at each time point of different friction times, five different

points were randomly selected for testing, and the average value of the paper contact angle was calculated.

■ ASSOCIATED CONTENT

Ⓢ Supporting Information

The Supporting Information is available free of charge at https://pubs.acs.org/doi/10.1021/acsomega.1c01861.

L*, *a**, and *b** values of the sample colors (PDF)

■ AUTHOR INFORMATION

Corresponding Author

Shangjie Jiang − *Faculty of Printing, Packaging Engineering and Digital Media Technology, Xi'an University of Technology, Xi'an 710048, P. R. China;* ⓞ orcid.org/0000-0003-1304-3395; Email: xautjsj@126.com

Authors

Shisheng Zhou − *Faculty of Printing, Packaging Engineering and Digital Media Technology, Xi'an University of Technology, Xi'an 710048, P. R. China*

Bin Du − *Faculty of Printing, Packaging Engineering and Digital Media Technology, Xi'an University of Technology, Xi'an 710048, P. R. China;* ⓞ orcid.org/0000-0003-1302-1348

Rubai Luo − *Faculty of Printing, Packaging Engineering and Digital Media Technology, Xi'an University of Technology, Xi'an 710048, P. R. China;* ⓞ orcid.org/0000-0002-9051-0885

Complete contact information is available at:
https://pubs.acs.org/10.1021/acsomega.1c01861

Notes

The authors declare no competing financial interest.

■ ACKNOWLEDGMENTS

■ REFERENCES

(1) Zhao, R.; Chen, Y.; Liu, G.; Jiang, Y.; Chen, K. Fabrication of Self-healing Waterbased Superhydrophobic Coatings from POSS modified Silica Nanoparticles. *Mater. Lett.* **2018**, *229*, 281−285.

(2) Liu, Z.; Wang, H.; Zhang, X.; Lv, C.; Zhao, Z.; Wang, C. Durable and self-healing superhydrophobic polyvinylidene fluoride (PVDF) composite coating with in-situ gas compensation function. *Surf. Coat. Technol.* **2017**, *327*, 18−24.

(3) Chen, K.; Zhou, S.; Wu, L. Self-Healing Underwater Super-oleophobic and Antibiofouling Coatings Based on the Assembly of Hierarchical Microgel Spheres. *ACS Nano* **2016**, *10*, 1386−1394.

(4) Manna, U.; Lynn, D. M. Synthetic Surfaces with Robust and Tunable Underwater Superoleophobicity. *Adv. Funct. Mater.* **2015**, *25*, 1672−1681.

(5) Liu, Z.; Yang, X.; Pang, G.; Zhang, F.; Han, Y.; Wang, X.; Liu, X.; Xue, L. Temperature-based adhesion tuning and superwettability

(6) Shang, Q.; Chen, J.; Liu, C.; Hu, Y.; Hu, L.; Yang, X.; Zhou, Y. Facile fabrication of environmentally friendly bio-based super-hydrophobic surfaces via UV-polymerization for self-cleaning and high efficient oil/water separation. *Prog. Org. Coat.* **2019**, *137*, 105346.

(7) Kakade, B.; Mehta, R.; Durge, A.; Kulkarni, S.; Pillai, V. Superhydrophobic to Superhydrophilic Switching in Multiwalled Carbon Nanotube Papers. *Nano Lett.* **2008**, *8*, 2693−2696.

(8) Chen, K.; Jia, J.; Zhao, Y.; Lv, K.; Wang, C. Transparent smart surface with pH-induced wettability transition between super-hydrophobicity and underwater superoleophobicity. *Mater. Des.* **2017**, *135*, 69−76.

(9) Li, Y.; Li, Q.; Zhang, C.; Cai, P.; Bai, N.; Xu, X. Intelligent self-healing superhydrophobic modification of cotton fabrics via surface-initiated ARGET ATRP of styrene. *Chem. Eng. J.* **2017**, *323*, 134−142.

(10) Chen, S.; Zhu, M.; Zhang, Y.; Dong, S.; Wang, X. Magnetic-Responsive Superhydrophobic Surface of Magnetorheological Elas-tomers Mimicking from Lotus Leaves to Rose Petals. *Langmuir* **2021**, *37*, 2312−2321.

(11) Ezazi, M.; Shrestha, B.; Klein, N.; Lee, D. H.; Seo, S.; Kwon, G. Self-Healable Superomniphobic Surfaces for Corrosion Protection. *ACS Appl. Mater. Interfaces* **2019**, *11*, 30240−30246.

(12) Qahtan, T. F.; Gondal, M. A.; Dastageer, M. A.; Kwon, G.; Ezazi, M.; Al-Kuban, M. Z. Thermally Sensitized Membranes for Crude Oil−Water Remediation under Visible Light. *ACS Appl. Mater. Interfaces* **2020**, *12*, 48572−48579.

(13) Ezazi, M.; Shrestha, B.; Kim, S. I.; Jeong, B.; Gorney, J.; Hutchison, K.; Lee, D. H.; Kwon, G. Selective Wettability Membrane for Continuous Oil-Water Separation and In Situ Visible Light-Driven Photocatalytic Purification of Water. *Global Challenges* **2020**, *4*, 2000009.

(14) Yang, X.; Zhuang, K.; Lu, Y.; Wang, X. Creation of Topological Ultraslippery Surfaces for Droplet Motion Control. *ACS Nano* **2021**, *15*, 2589−2599.

(15) Kato, S.; Sato, A. Micro/nanotextured polymer coatings fabricated by UV curing-induced phase separation: creation of superhydrophobic surfaces. *J. Mater. Chem.* **2012**, *22*, 8613−8621.

(16) Ye, X.; Hou, J.; Cai, D. Novel reversibly switchable wettability of superhydrophobic−superhydrophilic surfaces induced by charge injection and heating. *Beilstein J. Nanotechnol.* **2019**, *10*, 840−847.

(17) Jiang, C.; Liu, W.; Yang, M.; Liu, C.; He, S.; Xie, Y.; Wang, Z. Robust multifunctional superhydrophobic fabric with UV induced reversible wettability, photocatalytic self-cleaning property, and oil-water separation via thiol-ene click chemistry. *Appl. Surf. Sci.* **2019**, *463*, 34−44.

(18) Li, H.; Xin, B.; Feng, L.; Hao, J. Stable ZnO/ionic liquid hybrid materials: novel dual-responsive superhydrophobic layers to light and anions. *Sci. China: Chem.* **2014**, *57*, 1002−1009.

(19) Zhang, R.; Hao, P.; Zhang, X.; He, F. Supercooled water droplet impact on superhydrophobic surfaces with various roughness and temperature. *Int. J. Heat Mass Transfer* **2018**, *122*, 395−402.

(20) Yi, N.; Huang, B.; Dong, L.; Quan, X.; Hong, F.; Tao, P.; Song, C.; Shang, W.; Deng, T. Temperature-Induced Coalescence of Colliding Binary Droplets on Superhydrophobic Surface. *Sci. Rep.* **2014**, *4*, 4303.

(21) Clavijo, C. E.; Stevens, K.; Crockett, J.; Maynes, D. Thermally induced atomization during droplet impingement on superheated hydrophobic and superhydrophobic surfaces. *Int. J. Heat Mass Transfer* **2018**, *126*, 1357−1366.

(22) Chagas, G. R.; Weibel, D. E. UV-induced switchable wettability between superhydrophobic and superhydrophilic polypropylene surfaces with an improvement of adhesion properties. *Polym. Bull.* **2017**, *74*, 1965−1978.

(23) Hu, S.; Cao, X.; Song, Y.; Li, C.; Xie, P.; Jiang, L. New responsive property of poly (e-caprolactone) as the thermal switch from superhydrophobic to superhydrophilic. *Chem. Commun.* **2008**, *17*, 2025−2027.

(24) Xu, Z.; Zhao, Y.; Wang, H.; Zhou, H.; Qin, C.; Wang, X.; Lin, T. Fluorine-Free Superhydrophobic Coatings with pH-induced Wettability Transition for Controllable Oil−Water Separation. *ACS Appl. Mater. Interfaces* **2016**, *8*, 5661−5667.

(25) Sun, T.; Wang, G.; Feng, L.; Liu, B.; Ma, Y.; Jiang, L.; Zhu, D. Reversible Switching between Superhydrophilicity and Superhydrophobicity. *Angew. Chem., Int. Ed.* **2004**, *43*, 357−360.

(26) Lim, H. S.; Lee, W. H.; Lee, S. G.; Lee, D.; Jeon, S.; Cho, K. Effect of nanostructure on the surface dipole moment of photo-reversibly tunable superhydrophobic surfaces. *Chem. Commun.* **2010**, *46*, 4336−4338.

(27) Sun, W.; Zhou, S.; Chen, P.; Peng, L. Reversible switching on superhydrophobic TiO2 nano-strawberry films fabricated at low temperature. *Chem. Commun.* **2008**, *8*, 603−605.

(28) Jiang, C.; Liu, W.; Yang, M.; Liu, C.; He, S.; Xie, Y.; Wang, Z. Facile fabrication of robust fluorine-free self-cleaning cotton textiles with superhydrophobicity, photocatalytic activity, and UV durability. *Colloids Surf., A* **2018**, *559*, 235−242.

(29) Teng, Y.; Wang, Y.; Shi, B.; Chen, Y. Facile preparation of economical, eco-friendly superhydrophobic surface on paper substrate with excellent mechanical durability. *Prog. Org. Coat.* **2020**, *147*, 105877.

(30) Yokoi, N.; Manabe, K.; Tenjimbayashi, M.; Shiratori, S. Optically Transparent Superhydrophobic Surfaces with Enhanced Mechanical Abrasion Resistance Enabled by Mesh Structure. *ACS Appl. Mater. Interfaces* **2015**, *7*, 4809−4816.

(31) Ogihara, H.; Xie, J.; Okagaki, J.; Saji, T. Simple Method for Preparing Superhydrophobic Paper: Spray-Deposited Hydrophobic Silica Nanoparticle Coatings Exhibit High Water-Repellency and Transparency. *Langmuir* **2012**, *28*, 4605−4608.

(32) Jiang, S.; Zhou, S.; Du, B.; Luo, R. A study on the stability of superhydrophobic paper reinforced by amino-assisted modified PHFMA-PTSPM polymer. *Mater. Res. Express* **2020**, *7*, 105301.

(33) Zhang, Q.; Jin, B.; Wang, B.; Fu, Y.; Zhan, X.; Chen, F. Fabrication of a Highly Stable Superhydrophobic Surface with Dual-Scale Structure and Its Antifrosting Properties. *Ind. Eng. Chem. Res.* **2017**, *56*, 2754−2763.

(34) Fu, Y.; Jiang, J.; Zhang, Q.; Zhan, X.; Chen, F. Robust liquid-repellent coatings based on polymer nanoparticles with excellent self-cleaning and antibacterial performances. *J. Mater. Chem. A* **2017**, *5*, 275−284.

(35) Jiang, S.; Zhou, S.; Du, B.; Luo, R. Preparation of superhydrophobic paper with double-size silica particles modified by amino and epoxy groups. *AIP Adv.* **2021**, *11*, 025127.

(36) Ma, Y.; Cao, C.; Hou, C. *Preparation of Super-Hydrophobic Cotton Fabric with Crosslinkable Fluoropolymer*; Springer, 2018; pp 155−262.

(37) Park, J.-H.; Jang, J.-W.; Sim, J.-H.; Kim, I.-J.; Lee, D.-J.; Lee, Y.-H.; Park, S.-H.; Kim, H.-D. Preparation and Properties of Thermoresponsive P (N-Isopropylacrylamide-co-butylacrylate) Hydrogel Materials for Smart Windows. *Int. J. Polym. Sci.* **2019**, *2019*, 3824207.

(38) Jain, A.; Bajpai, J.; Bajpai, A. K.; Mishra, A. Thermoresponsive cryogels of poly (2-hydroxyethyl methacrylate-co-N-isopropyl acryl-amide) (P (HEMA-co-NIPAM)): fabrication, characterization and water sorption study. *Polym. Bull.* **2020**, *77*, 4417−4443.

(39) Du, B.; Xue, D.; Luo, R.; Li, H.; Yang, K.; Zhou, S. Preparation of Fluorine-Free Superhydrophobic Paper with Dual-Response of Temperature and pH. *Coatings* **2020**, *10*, 1167.

(40) Ishida, N.; Biggs, S. Effect of Grafting Density on Phase Transition Behavior for Poly (N-isopropylacryamide) Brushes in Aqueous Solutions Studied by AFM and QCM-D. *Macromolecules* **2010**, *43*, 7269−7276.

(41) Lin, S.-Y.; Chen, K.-S.; Liang, R.-C. Thermal micro ATR/FT-IR spectroscopic system for quantitative study of the molecular structure of poly(N-isopropylacrylamide) in water. *Polymer* **1999**, *40*, 2619−2624.

(42) Du, B.; Chen, F.; Luo, R.; Li, H.; Zhou, S.; Liu, S.; Hu, J. Superhydrophobic Surfaces with pH-Induced Switchable Wettability for Oil−Water Separation. *ACS Omega* **2019**, *4*, 16508−16516.